

**IN SITU ANALYSES OF CARBONATE AND MAGNETITE IN CM1 CHONDRITES.** M. Telus, C. M. O'D. Alexander, J. Wang, E. H. Hauri, DTM, Carnegie Institution of Washington, Washington, D.C. 20015 [mtelus@carnegiescience.edu](mailto:mtelus@carnegiescience.edu).

**Introduction:** CM chondrites exhibit a wide range in degrees of aqueous alteration, providing the tools to constrain the role of fluids in the formation and the early evolution of planetesimals. Here, we present the results of in situ C and O isotope analyses of calcite and dolomite, and O isotope analyses of magnetite from three highly altered CM1 chondrites. These chondrites may have formed in the interior, hotter, regions of the CM chondrite parent body [1].

**Samples:** We have analyzed calcite, dolomite and/or magnetite in the CM1 chondrites, ALH 84034, ALH 83100, and MET 01070. The ALH samples may be paired. All three have been analyzed for bulk D/H and bulk carbonate C and O isotope compositions [2, 3]. For ALH 84034, we analyzed 9 calcite, 10 dolomite, and 5 magnetite grains. We analyzed 12 calcite, 11 dolomite and 5 magnetite grains from ALH 83100 and for MET 01070, we analyzed 40 calcite grains and 4 dolomite grains, but no magnetite grains. All three samples are breccias. Large ( $>10\ \mu\text{m}$ ) dolomite grains are abundant in the ALH samples, but rare in MET 01070. Magnetite is rare in all three samples and dispersed sporadically in the matrix. The samples were characterized before and after isotope analyses using Carnegie's JEOL 6500 FE SEM and/or the JEOL 8530F electron microprobe.

**Isotope analyses:** In situ C and O isotope analyses were carried out using Carnegie's NanoSIMS 50L with a  $\text{Cs}^+$  primary beam of  $\sim 70\text{-}100\ \text{pA}$  [4]. Real-time images were checked before and after each analysis to ensure that cracks or multiple phases were not included in the analyzed areas. Analyses of areas with cracks, etc., were discarded. Sample-standard bracketing with terrestrial carbonate and magnetite standards was used to correct for drift in the EMs and instrumental mass fractionation (IMF). The uncertainties in the isotope ratios include errors from the IMF corrections and counting statistics.

**Results:** The C and O isotope data for all the analyses are shown in Figure 1, and the  $\Delta^{17}\text{O}$  values are shown in Figure 2. All the reported uncertainties are  $1\sigma$ . The data for  $\delta^{13}\text{C}$  vs.  $\delta^{18}\text{O}$  fall into two arrays, one consisting of only calcite with relatively low  $\delta^{13}\text{C}$  and high  $\delta^{18}\text{O}$  values, and the other consisting of dolomite and calcite with relatively high  $\delta^{13}\text{C}$  and low  $\delta^{18}\text{O}$  values (Fig. 1, right).

Dolomites from all three chondrites have similar  $\delta^{13}\text{C}$  and  $\delta^{18}\text{O}$  compositions. For the ALH samples, the dolomite is systematically enriched in  $^{13}\text{C}$  relative to calcite. The  $\delta^{13}\text{C}$  compositions of calcite and dolomite

in ALH 84034 have relatively homogeneous values of  $\sim 27\text{‰}$  and  $\sim 53\text{‰}$ , respectively, but a range in  $\delta^{18}\text{O}$ . Dolomites in ALH 83100 are homogeneous in  $\delta^{13}\text{C}$  and  $\delta^{18}\text{O}$ , while the calcite shows a spread in  $\delta^{13}\text{C}$  and  $\delta^{18}\text{O}$  values. For MET 01070, the calcite compositions are bimodal: both populations are enriched in the heavy O isotopes relative to dolomite, but one population has  $\delta^{13}\text{C}$  (50-80‰) that is higher than those for dolomite; while the other has  $\delta^{13}\text{C}$  slightly lower than dolomite (30-50‰).

For ALH 84034, the  $\Delta^{17}\text{O}$  values for calcite, dolomite, and magnetite span a wide range. The calcite composition ranges from  $-9\text{‰}$  to  $+5\text{‰}$ , dolomite spans from  $-6\text{‰}$  to  $+7\text{‰}$ , and that for magnetite ranges from  $-9\text{‰}$  to  $-2\text{‰}$ . The  $\Delta^{17}\text{O}$  values for calcite, dolomite and magnetite from ALH 83100 have a more limited range between  $-3\text{‰}$  and  $+4\text{‰}$ . The  $\Delta^{17}\text{O}$  values of calcite from MET 01070 are mostly below zero. The dolomite analyses were few, but span a very wide range.

**Discussion:** These chondrites exhibit large variations in their carbonate and magnetite O-isotope compositions on small spatial scales, suggesting that local conditions in the parent body controlled the extent of aqueous alteration. The measured dolomite-calcite O-isotope fractionation is much larger than what is expected for equilibrium fractionation [5]. It is clear from the petrology that dolomite formed after calcite in all of these chondrites. Dolomite is systematically enriched in  $^{16}\text{O}$  compared to calcite, supporting progressive alteration in a localized closed system [e.g., 1].

Homogeneous  $\Delta^{17}\text{O}$  values for secondary minerals in ALH 83100 indicate little change in the fluid composition with progressive alteration possibly due to large water-to-rock ratios for this sample.

Secondary minerals in ALH 84034 exhibit a wide range in  $\Delta^{17}\text{O}$  values, including the most positive values among the three chondrites analyzed here. The positive  $\Delta^{17}\text{O}$  values are significant because primordial water had positive  $\Delta^{17}\text{O}$  [e.g., 6], suggesting that the fluid that interacted with ALH 84034 may have been isotopically more pristine compared to the others. Interestingly, dolomite, which formed after calcite, has some of the most positive  $\Delta^{17}\text{O}$  values, inconsistent with progressive alteration in closed system. The positive  $\Delta^{17}\text{O}$  values may support the fluid flow model proposed by [7], but on a much smaller scale.

Calcite and magnetite formation in carbonaceous chondrites may have occurred in equilibrium [8]. The measured fractionation between calcite and magnetite in ALH 84034 and ALH 83100 is  $\sim 25\text{‰}$  and  $33\text{‰}$ ,

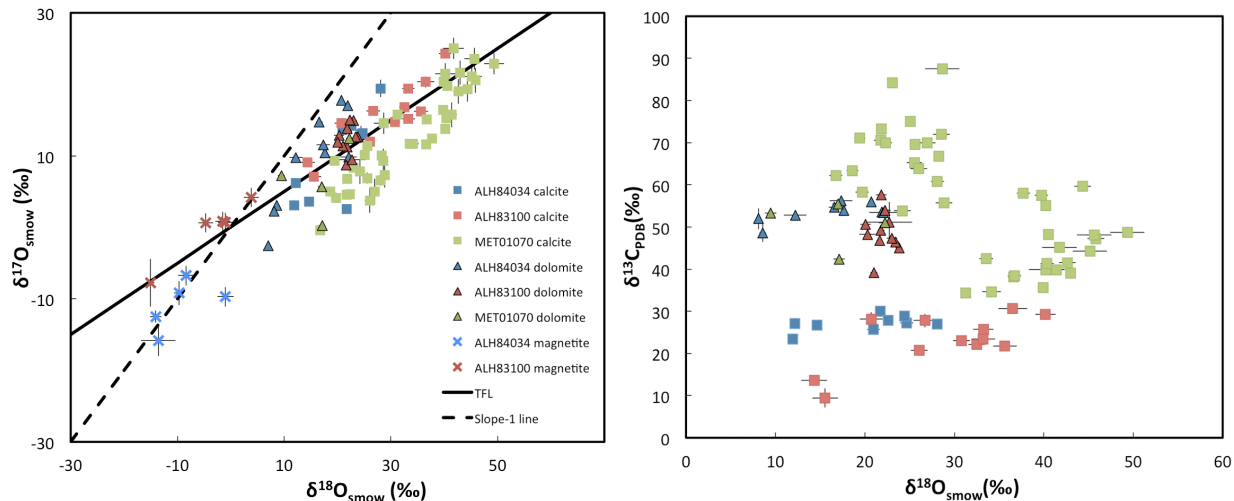


Figure 1.  $\delta^{17}\text{O}$  vs.  $\delta^{18}\text{O}$  (left) and  $\delta^{13}\text{C}$  vs.  $\delta^{18}\text{O}$  (right) of calcite (squares), dolomite (triangles) and magnetite (crosses) for CM1 chondrites ALH 84034 (blue), ALH 83100 (red) MET 01070 (green). Errors are  $1\sigma$ .

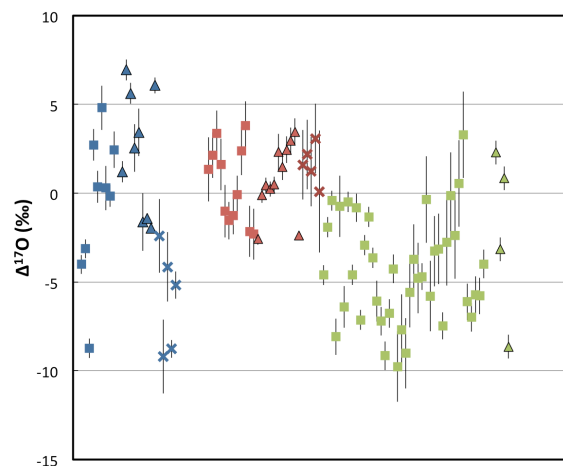


Figure 2.  $\Delta^{17}\text{O}$  values with  $1\sigma$  uncertainties. There are large variations between the three chondrites.

respectively, corresponding to precipitation at 80 °C and 30 °C, respectively [9]. This range in temperature is consistent with estimates from clumped isotope thermometry [10].

The dolomite-calcite  $\delta^{13}\text{C}$  fractionation is much larger than what is expected for equilibrium fractionation. Calcite in MET 01070 falls into two isotopic groups, one group has  $\delta^{13}\text{C}$  values similar to dolomite. Cathodoluminescence petrography shows that this group of calcite grains formed later as it occurs predominately on the periphery of the  $^{13}\text{C}$ -depleted calcite grains. Thus, progressive alteration results in secondary minerals becoming enriched in  $^{13}\text{C}$ . This  $\sim 30\text{‰}$  shift in  $\delta^{13}\text{C}$  may relate to a drastic change in the concentration of  $\text{CO}_2$  in equilibrium with the fluid [3]. If so, the model from [3] indicates that the concentration

of  $\text{CO}_2$  suddenly became depleted in  $^{13}\text{C}$  prior to dolomite formation or precipitation of  $^{13}\text{C}$ -enriched calcite in MET 01070. This dramatic shift in  $\delta^{13}\text{C}$  may be an isotopic signature of venting due to pressure build-up on the parent body [11]. The  $^{53}\text{Mn}$ - $^{53}\text{Cr}$  ages for dolomite in CM1s [e.g., 12] may be recording this venting event.

**Conclusions:** We analyzed C and O in situ for carbonates and/or magnetite in CM1 chondrites to piece together the details regarding aqueous alteration of the CM chondrite parent body. Our data support both locally closed- and open-system aqueous alteration and provides isotopic evidence for secondary mineral precipitation during venting, or the release of water vapor pressure build-up on the parent body.

**References:** [1] Clayton R. N. and Mayeda T. K. 1984. *EPSL*, 67, 151-161. [2] Alexander C. M. O'D. et al. 2013. *GCA*, 123, 244-260. [3] Alexander C. M. O'D. 2015. *MAPS*, 50: 810-833. [4] Telus M. et al. 2015. *MAPS*, abstract #5395. [5] Horita J. 2014. *GCA*, 129, 111-124. [6] Sakamoto, N., et al. 2007. *Science*, 317, 231-233. [7] Young E. D., et al. (1999). *Science*, 286, 1331-1335 [8] Jilly C. E. et al., 2014. *MAPS*, abstract #6498. [9] Feng Y.-F. 1995. *Chem. Geol.*, 121, 309-316. [10] Guo W. and Eiler J. M. 2007. *GCA*, 71, 5565-5575. [11] Grimm R. E. and McSween H. Y. 1989. *ICARUS*, 82, 244-280. [12] Tyra M., et al. 2016. *GCA*, 175, 195-207.

*Many thanks to K.D. McKeegan (UCLA) and J.G. Wynn (USF) for the terrestrial standards and thanks to the Carnegie Postdoctoral Fellowship for funding.*